SPEKTRA: Jurnal Fisika dan Aplikasinya
Volume 9, Issue 2, August 2024
Homepage: doi.org/10.21009/SPEKTRA

DOI: doi.org/10.21009/SPEKTRA.092.03

Enhanced Approaches to Gravitational Lensing: A Regular Charged Black Hole in Weak Field Limit

H. M. U. Din*, H. S. Ramadhan

Department Fisika, FMIPA, Universitas Indonesia, Depok, 16424, Indonesia

*Corresponding Author Email: hassan.moin@ui.ac.id

Received: 9 June 2024
Revised: 12 July 2024
Accepted: 13 July 2024
Online: 22 July 2024
Published: 30 August 2024

SPEKTRA: Jurnal Fisika dan Aplikasinya
p-ISSN: 2541-3384
e-ISSN: 2541-3392

ABSTRACT

Gravitational lensing, an integral aspect of general relativity, profoundly impacts our understanding of black holes (BH's). The presence of a centered singularity resulting from gravitational collapse is a fundamental characteristic of a BH. Nonetheless, the exploitation of non-linear electrodynamics (NLED) divulges the emphatic concept of non-singularity. Our analysis primarily focuses on calculating the deflection angle in the weak field approximation, deliberately excluding the original spacetime configuration. The photon's effective geometry is typically linked to NLED. Instead, a photon traverses an effective null geodesic that aligns with the geometry of a regular metric. The findings reveal an additional term in the deflection angle compared to the Reissner-Nordström (RN) metric, evidenced by a shifted positional displacement of the tertiary image associated with a regular BH. This study succinctly encapsulates these findings, positioning them within the extensive terminology ambient to BH's singularity and GL, thus edifying the scientific memoir with precise astrophysical insights.

Keywords: gravitational lensing, weak field limit, image position, magnification

INTRODUCTION

Gravitational lensing emerges as a consequence of the General Theory of Relativity (GR), and it predicts the existence of black holes by solving Einstein Field Equations (EFE). Thorough scrutiny of celestial phenomena provided evidence of the imminent existence of supermassive BH's in the cosmos. The latest possible innovation made by Event Horizon Telescope (EHT) constructed an inconceivable supermassive BH centering in the giant galaxy M87 and Sagittarius A* (our Milky Way Galaxy's esoteric core) [1][2]. However, meticulous observations elucidate unrivaled glimpses of the outer visible BH. Contrarily, the enclosing mysterious inside of it is not known yet at all. The continuously inward spacetime described by standard solutions, i.e., Schwarzschild and Reissner-Nordström, ends in an inevitable singularity [3][4]. To avoid this inherited singularity, the regular perspective [5][6] of a charged BH is offered by the coupling approach of GR to NLED along with the electric charge. Regular BH's are theoretical entities characterized by the absence of singularities [7][8] within their core, thus preserving the determinism of physical laws even at the heart of these extreme objects. The NLED framework is very important in coming up with the idea of regular BH, in which changes to Maxwell's equations coupling with EFE's effectively reduce the infinite curvature [9][10]. This transforms a BH's central singularity into a spacetime geometry that is both finite and continuous. This theoretical framework allows for the mitigation of the infinite curvature typically associated with BH cores. Besides, by implying NLED, the scalar invariants, and the electric fields become regular everywhere [11][12]. Recently, numerous significant attempts have been made to ascertain lensing by electrically charged BH's. The pioneering initiative by Fernando [13] established a unique strategy to calculate the angular deviation of light by a variety of spherically symmetric charged black holes, especially for standard RN. Furthermore, the study by Eiroa and Sendra [14] delves into gravitational lensing by regular black holes, revealing crucial aspects of image positions and magnifications in such contexts.

In this paper, weak gravitational lensing using a regular-charged black hole has been investigated, and its distinctive behavior compared to the Reissner-Nordström black hole has been explained in terms of the deflection angles, angular image positions, and magnification properties. Furthermore, the formalism of a regular charge is interpreted, followed by a narration of the theoretical approach for calculating the deflection angle. Subsequently, the results are discussed briefly, and finally, the conclusion is presented.

A REGULAR CHARGED BLACK HOLE

The most general form of line element for homogeneous and isotropic spacetime is written as

$$\mathrm{d}s^2 = c^2 f(r)\mathrm{d}t^2 - g(r)\mathrm{d}t^2 - h(r)(\mathrm{d}\theta^2 + \sin^2\theta\,\mathrm{d}\phi^2). \tag{1}$$

Keep the constant c (speed of light) = 1, and use mass as a function of r, i.e., $m = m(r)$,

$$f(r) = 1 - \frac{2m(r)}{r}, \tag{2}$$

$$g(r) = 1 + \frac{2m(r)}{r}, \tag{3}$$

$$h(r) = r\,. \tag{4}$$

The electric fields and scalar curvature invariants of a regular BH are regular as long as r is greater than the event horizon radius. These are the Kretschmann scalar $K = R_{\rho\sigma\mu\nu}R_{\rho\sigma\nu\mu}$ and the Ricci scalar $R_{\rho\sigma} = R_{\lambda\rho\lambda\sigma}$, respectively [15]. Its mass function, $m(r)$, further corresponds to:

$$m(r) = \frac{\sigma(r)}{\sigma(\infty)}M\,, \tag{5}$$

where $\sigma(r)$ is the distribution function, and it should satisfy the following conditions as well:

$$\left.\begin{array}{l}\sigma(r) > 0 \\ \sigma^{'}(r) > 0\end{array}\right\} \text{at } r \geq 0.$$

Pursuing Veganas' models of regular BH's [16], the corresponding distribution function used is,

$$\sigma(r) = e^{-\sqrt{\frac{2Q^2}{Mr}}\left(1+-\sqrt{\frac{2Q^2}{Mr}}\right)^{-2}}. \tag{6}$$

In this case, the normalization factor, i.e., at $r = \infty \rightarrow \sigma(r) = \sigma(\infty)$ approaches 1/4. Asymptotically, a regular charged BH tends to the original RN solution by expanding the exponential function up to the first in the power development series with respect to r,

$$f(r) = 1 - \frac{2M(r)}{r} \approx 1 - \frac{2M}{r} + \frac{Q^2}{r^2}. \tag{7}$$

Here, the extremal electric charge value for this kind of BH is $|Q| = 1.055M$.

LIGHT DEFLECTION BY A SPHERICALLY SYMMETRIC MASS

To calculate the deflection angle in terms of metric for a static and isotropic weak field, one can formulate the light equation of motion from the following form of the null geodesic,

$$\frac{g(r)}{r^4}\left(\frac{\mathrm{d}r}{\mathrm{d}\phi}\right)^2 - \frac{1}{f(r)p^2} + \frac{1}{r^2} = 0\,. \tag{8}$$

FIGURE 1 illustrates the trajectory of the light ray coming from infinity with some impact parameter p and at a certain closest approach a to the mass. Due to the constant nature of a, the term $\frac{\mathrm{d}a}{\mathrm{d}\phi}$ vanishes, producing a relation such as,

$$p(a) = a\big(f(r)\big)^{-\frac{1}{2}}. \tag{9}$$

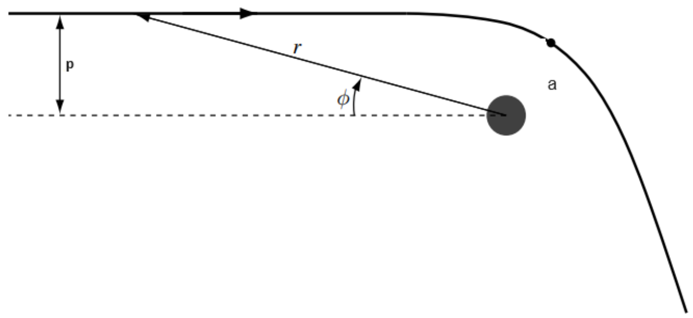

FIGURE 1. Illustration of light bending when it passes near a mass at a specific closest approach

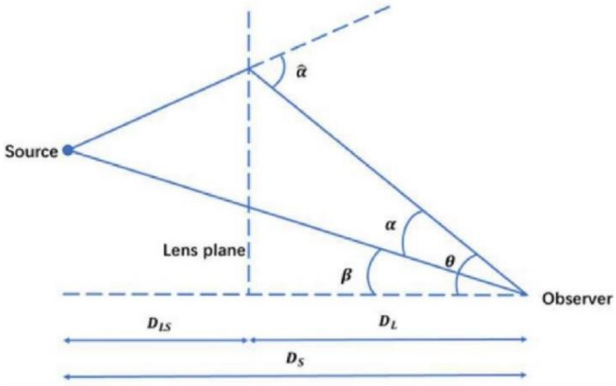

FIGURE 2. Simplest lensing geometric view [17]

The configuration of gravitational lensing is represented geometrically in FIGURE 2. By using the asymptotes corresponding to the differential form of the orbital equation, one can write the angle of deflection in terms of $\phi(r)$,

$$\phi = \pm\left(\frac{\pi}{2} + \delta\right) ; \qquad \hat{\alpha} = 2|\phi(r) - \phi(\infty)| - \pi.$$

Here, $\phi(\infty)$ is at spatial infinity, where the gravitational field is expected to be zero, and $\phi(r)$ represents a certain distance r from the trajectory of a light ray to the mass. Factor 2 ensures that the light ray deflects both upon approach and departure from the mass. Subtracting π indicates the fact that it might be a straight line if it comes out as a π. Finally, the total deflection angle [18][19] in terms of metric is as follows:

$$\hat{\alpha} = 2\int_a^\infty g^{\frac{1}{2}}(r)\left[\frac{f(a)}{f(r)}\left(\frac{r^2}{a^2}\right) - 1\right]^{-\frac{1}{2}} \frac{dr}{a} - \pi. \tag{10}$$

Integrating EQUATION (10) results in divergence. To avoid it, the metric function has been improvised (as discussed in the next section). From the geometry view, as given in FIGURE 2, the angular image positions can be calculated with the help of a lens equation. The thin-lens approximation is a reduced form that represents an unaltered, direct path of the light rays that are subject to weak or not at all gravitational distortion. The lens equation relating the observable image positions to the source positions is

$$\beta = \theta - \hat{\alpha}\frac{D_{ls}}{D_s}, \tag{11}$$

where D_{ds} is the lens source distance, β is the angular position of the source, and θ is the angular image position of the image. The event horizon has a weaker influence on the light ray if one considers it to pass farther away from the mass with a greater impact parameter. The latter justifies the thin-lens approximation. Under the same scenario, calculations have been done for Schwarzschild in WFL. Further, one can assume the impact parameter equals or is close to the closest approach in the WFL. The ratio between the angles of the source and an image accounts for the magnification property (conserving the luminosity of the surface). In addition to measuring the image positions, the following expression could be used to observe the magnification characteristics:

$$\mu = \frac{d\theta}{d\beta}\frac{\theta}{\beta}. \tag{12}$$

RESULTS AND DISCUSSION

Enhanced approaches in WFL were applied by expanding the metric and exponential functions up to the fourth order (one can use any other higher than two). Then,

$$\frac{f(a)}{f(r)} \approx \left(1 - \frac{2M}{a} + \frac{Q^2}{a^2} - \frac{5Q^4}{12Ma^3}\right)\left(1 + \frac{2M}{r} + \frac{4M^2}{r^2} - \frac{Q^2}{r^2} + \frac{8M^3}{r^3} - \frac{4MQ^2}{r^3} + \frac{5Q^4}{12Mr^3}\right)$$

and

$$\begin{aligned}
&\left[\frac{f(a)}{f(r)}\left(\frac{r^2}{a^2}\right) - 1\right]\left[\frac{r^2}{a^2} - 1\right]^{-1} \\
&\quad = \frac{1}{180a^4M^2r^2(a + r)}[180a^5M^2r^2 + 180a^4M^2r^3 + 17Q^6r^3 \\
&\quad + aQ^4r^2\{17Q^2 - 120M^2 - 60Mr\} \\
&\quad + a^2\{720M^4 + 17Q^4 + 360M^3r - 60M^2 - 60MQ^2r(5Q^2 - 3r^2)\} \\
&\quad - a^3\{-17Q^6 + 2880M^6 + 1440M^5r + 60MQ^4r - 720M^4) \\
&\quad + 60M^2(7Q^4 - 3Q^2r^2) - 360M^3(2Q^2r - r^3)\}],
\end{aligned} \tag{13}$$

were obtained.

Finally, the deflection angle of a regular charged BH w.r.t. the closest approach in weak field limit can be written as follows:

$$\begin{aligned}
\hat{\alpha} = &\frac{4M}{a} + \frac{M^2}{4a^2}\left(-4 + \frac{15\pi}{4}\right) - \frac{3\pi Q^2}{4a^2} - \frac{M^3}{a^3}\left(36 - \frac{15\pi}{2}\right) + \frac{MQ^2}{a^3}\left(-14 + \frac{3\pi}{2}\right) \\
&+ \frac{M^4}{a^4}\left(-\frac{434}{4} + \frac{3465\pi}{64}\right) + \frac{M^2Q^2}{a^4}\left(50 - \frac{825\pi}{32}\right) + \frac{57\pi Q^4}{64a^4} - \frac{17\pi Q^6}{192a^4M^2}.
\end{aligned} \tag{14}$$

Here, $17\pi Q^6/192a^4M^2$ is found to be an additional term in the deflection angle of a regular charged BH. This is the term which makes a regular BH distinct than RN in terms of deflection angle [20][21]. Besides numerically, this difference in deflection angles w.r.t. the impact parameter can also be seen graphically, as given in FIGURE 3, along with the graphical view of the additional term appearing in EQUATION (14) presented in FIGURE 4. Moreover, one can also reflect on the relation of how the deflection angle of a regular BH behaves depending on the electric charge Q (given in FIGURE 5).

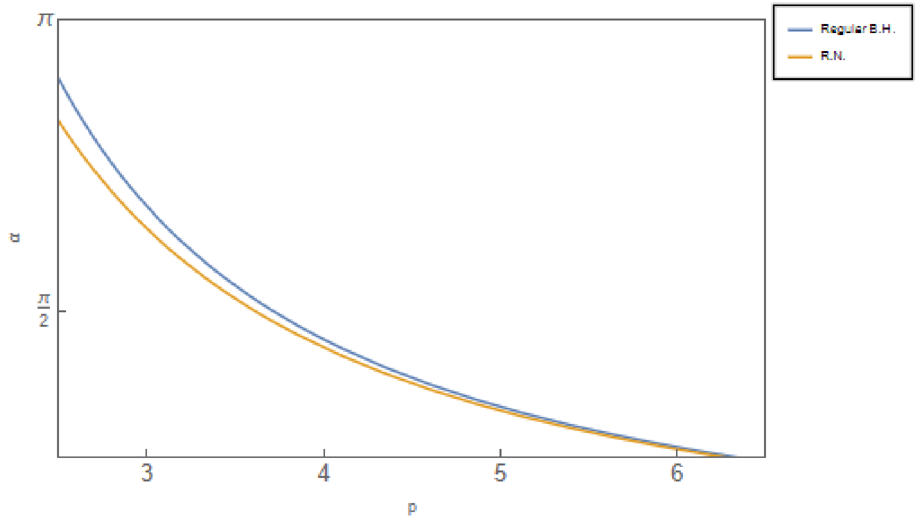

FIGURE 3. Deflection angle vs. impact parameter

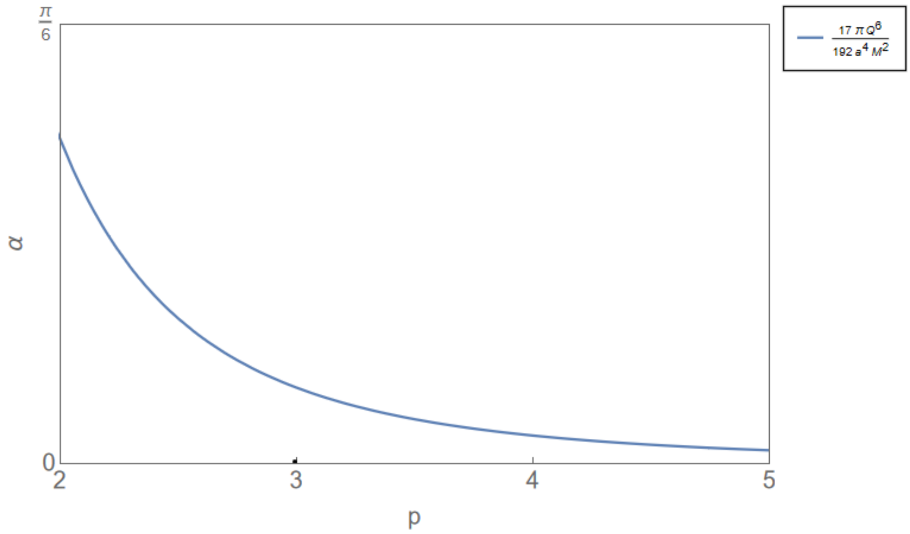

FIGURE 4. Additional term in deflection angle of a regular charged BH

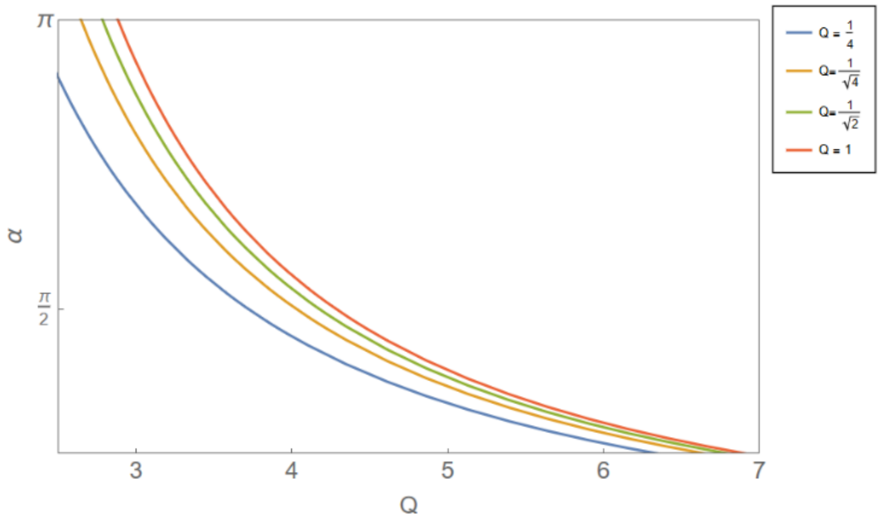

FIGURE 5. Deflection angle vs. electric charge

TABLE 1. Three angular image positions

Regular Black Hole				Reissner-Nordström Black Hole		
β	First Image	Second Image	Third Image	First Image	Second Image	Third Image
10^{-4}	-1.15577	1.15587	-4.91901×10^{-6}	-1.15577	1.15587	-5.02259×10^{-6}
10^{-3}	-1.15532	1.15632	-4.91901×10^{-6}	-1.15532	1.15632	-5.02259×10^{-6}
10^{-2}	-1.15083	1.16083	-4.91901×10^{-6}	-1.15083	1.16083	-5.02259×10^{-6}
10^{-1}	-1.10690	1.20690	-4.91901×10^{-6}	-1.10690	1.20690	-5.02259×10^{-6}
1	-0.75933	1.75933	-4.91902×10^{-6}	-0.75933	1.75933	-5.0226×10^{-6}
2	-0.52837	2.52837	-4.91903×10^{-6}	-0.52837	2.52837	-5.02261×10^{-6}
3	-0.39367	3.39365	-4.91905×10^{-6}	-0.39367	3.39365	-5.02262×10^{-6}
4	-0.30996	4.30996	-4.91906×10^{-6}	-0.30996	4.30996	-5.02263×10^{-6}
5	-0.25425	5.25425	-4.91907×10^{-6}	-0.25425	5.25425	-5.02264×10^{-6}

Pursuing further, the angular image positions of a regular charged BH have been measured by following EQUATION (11). To do so, a few of the parameters [22][23] are suggested, as follows: the mass of a supermassive BH is taken as $M = 2.8 \times M_{\odot}$, the distance from BH to observe is $D_d = 8.5$ kpc, and the charge is $Q^2 = M^2/2$. Additionally, the ratio of the distance from the source to BH and the distance from BH to the observer was assumed to be $D_{ls}/D_l = 1/2$. TABLE 1 shows the comparable image positions of a regular BH w.r.t. RN.

Upon comparing the patterns with RN, the first and second images of a regular BH maintain the same positions despite the different source positions [24]. Only the third image exhibits noticeable shifts. It is interesting to note that the first and second images show continuous movement towards and away from the optical axis, respectively, as the source position increases. Nevertheless, the third image remains surprisingly stable and is very difficult to measure.

TABLE 2. Magnifications

Regular Black Hole				Reissner-Nordström Black Hole		
β	First Magnifi-cation	Second Magnifi-cation	Third Magnification	First Magnifi-cation	Second Magnifi-cation	Third Magnification
10^{-4}	5779.6	-5778.6	5.33164×10^{-13}	5779.6	-5778.6	5.64064×10^{-13}
10^{-3}	578.41	-577.41	5.33164×10^{-14}	578.41	-577.41	5.64064×10^{-14}
10^{-2}	58.2926	-57.2926	5.33164×10^{-15}	58.2926	-57.2926	5.64064×10^{-15}
10^{-1}	6.29531	-5.29531	5.33165×10^{-16}	6.29531	-5.29531	5.64064×10^{-16}
1	1.22892	-0.22893	5.33172×10^{-17}	1.22892	-0.22893	5.64072×10^{-17}
2	1.04567	-0.04567	2.6659×10^{-17}	1.04567	-0.04567	2.8204×10^{-17}
3	1.01364	-0.01364	1.77729×10^{-17}	1.01364	-0.01364	1.8803×10^{-17}
4	1.0052	-0.00520	1.33299×10^{-17}	1.0052	-0.00520	1.41024×10^{-17}
5	1.00235	-0.00235	1.06641×10^{-17}	1.00235	-0.00235	1.12821×10^{-17}

Regarding the comparison of the magnification properties with RN (given in TABLE 2), the configuration of the first and second images demonstrates no changes at all. While the effective luminosity diminishes with the increasing source position. Particularly, the third image illuminates' bit lower than that of regular-charged BH but is still too rigorous to measure.

When comparing the magnification properties with Reissner-Nordström BH (as shown in TABLE 3), the configuration of the first and second images shows no changes [25]. As the source position increases, subsequently, the effective brightness decreases. Interestingly, the third image is slightly less bright rather than a regular BH but remains too difficult to measure precisely.

CONCLUSION

It has been discerned that the general relativity coupling to NLED manifests an enhanced way to modify the behavior of black holes. An additional term appears while calculating the deflection angle of a regular charged BH in terms of metric. Such a term makes a regular BH distinct than standard Reissner-Nordström BH. This difference can be clearly observed both numerically and graphically. Meanwhile, the deflection angle w.r.t. impact parameter reveals that the angle of deflection always expands by decreasing the impact parameter. The presence of the electric charge in regular charged BH also reflects its behavior relative to the deflection angle, which possesses a similar pattern with RN, but the difference lies in different shifts. Moreover, due to the distinguishable terms in regular charged BH, various angular image positions and their magnifications were found, as compared to Reissner-Nordström.

REFERENCES

[1] Event Horizon Telescope Collaboration et al., "First M87 event horizon telescope results. I. The shadow of the supermassive black hole," *Astrophys. J. Lett.*, vol. 875, no. 1, 2019, doi: 10.3847/2041-8213/ab0ec7.

[2] Q. Wu, "The first black hole image: An introduction to black hole," *Chinese Journal of Nature*, vol. 41, no. 3, 2019, doi: 10.3969/j.issn.0253-9608.2019.03.001.

[3] R. Sharma and M. Sharma, "The origin of supermassive black holes at cosmic dawn," *Monthly Notices of the Royal Astronomical Society*, vol. 531, no. 3, 2024, doi: 10.1093/mnras/stae1007.

[4] L. Riofrio, "Black Hole Singularities and Planetary Formation," *Journal of Applied Mathematics and Physics*, vol. 12, no. 4, 2024, doi: 10.4236/jamp.2024.124067.

[5] K.-H. Spatschek, *Astrophysics: An Introduction to Theory and Basics*. Springer Nature, 2024.

[6] S. N. Sajadi and N. Riazi, "Nonlinear electrodynamics and regular black holes," *General Relativity and Gravitation*, vol. 49, no. 45, 2017, doi: 10.1007/s10714-017-2209-8.

[7] K. A. Bronnikov, "Regular black holes sourced by nonlinear electrodynamics," *Regular Black Holes: Towards a New Paradigm of Gravitational Collapse*, Springer Nature Singapore, 2023, doi: 10.1007/978-981-99-1596-5_2.

[8] A. Vijaykumar, *Exploring gravity, astrophysics, and cosmology with gravitational waves*, Ph.D. dissertation, Tata Institute of Fundamental Research, 2024. [Online]. Available: https://thesis.icts.res.in/sites/default/files/2024-03/Final%20thesis%20%285%29.pdf

[9] A. S. Habibina and H. S. Ramadhan, "Geodesic of nonlinear electrodynamics and stable photon orbits," *Physical Review D*, vol. 101, no. 12, 2020, doi: 10.1103/PhysRevD.101.124036.

[10] A. He et al., "Effects of Born–Infeld electrodynamics on black hole shadows," *The European Physical Journal C*, vol. 82, no. 8, 2022, doi: 10.1140/epjc/s10052-022-10637-x.

[11] E. Ayón-Beato and A. García, "Regular black hole in general relativity coupled to nonlinear electrodynamics," *Physical Review Letters*, vol. 80, pp. 5056-5059, 1998, doi: 10.1103/PhysRevLett.80.5056
[12] I. P. Denisova, B. D. Garmaev, and V. A. Sokolov, "Compact objects in conformal nonlinear electrodynamics," *The European Physical Journal C*, vol. 79, no. 531, 2019, doi: 10.1140/epjc/s10052-019-7044-5.
[13] S. Fernando and S. Roberts, "Gravitational lensing by charged black holes," *General Relativity and Gravitation*, vol. 34, pp. 1221–1230, 2002, doi: 10.1023/A:1019726501344.
[14] E. F. Eiroa and C. Sendra, "Gravitational lensing by a regular black hole," *Classical and Quantum Gravity*, vol. 28, no. 8, 2011, doi: 10.1088/0264-9381/28/8/085008.
[15] J. Y. Kim, "Deflection of light by a Coulomb charge in Born–Infeld electrodynamics," *The European Physical Journal C*, vol. 81, no. 508, 2021, doi: 10.1140/epjc/s10052-021-09291-6.
[16] L. Balart and E. C. Vagenas, "Regular black holes with a nonlinear electrodynamics source," *Physical Review D*, vol. 90, no. 12, 2014, doi: 10.1103/PhysRevD.90.124045.
[17] P. Bueno, P. A. Cano, and R. A. Hennigar, "Regular Black Holes From Pure Gravity," *arXiv preprint arXiv:2403.04827*, 2024, doi: 10.48550/arXiv.2403.04827.
[18] J. Zhang and Y. Xie, "Gravitational lensing by a black-bounce-Reissner–Nordström spacetime," *The European Physical Journal C*, vol. 82, no. 471, 2022, doi: 10.1140/epjc/s10052-022-10441-7.
[19] K. Umetsu, "Cluster–galaxy weak lensing," *The Astronomy and Astrophysics Review*, vol. 28, no. 7, 2020, doi: 10.1007/s00159-020-00129-w.
[20] W. Javed, A. Hamza, and A. Övgün, "Effect of nonlinear electrodynamics on the weak field deflection angle by a black hole," *Physical Review D*, vol. 101, no. 10, 2020, doi: 10.1103/PhysRevD.101.103521.
[21] E. Dil, "Semi-classical gravitational lensing near a black hole," *Indian Journal of Physics*, vol. 96, pp. 1277–1281, 2022, doi: 10.1007/s12648-021-02033-0.
[22] Q. Qi et al., "Gravitational lensing effects of black hole with conformally coupled scalar hair," *The European Physical Journal C*, vol. 83, no. 1043, 2023, doi: 10.1140/epjc/s10052-023-12233-z.
[23] E. Vaynberg, *The Light of the Dark: Dark Matter, Astronomy, and Knowing the Unobservable*, Ph.D. dissertation, University of Pennsylvania, 2024. [Online]. Available: https://repository.upenn.edu/handle/20.500.14332/60172
[24] F. T. Hioe, "Characterizing planetary orbits and trajectories of light in the Reissner-Nordström metric," in *General Relativistic Effects and Elliptic Functions*, Cambridge Scholar Publishing, 2024, pp. 119. [Online]. Available: Google Books.
[25] B. N. Barlow et al., "Hot subdwarfs in close binaries observed from space-III. Reflection effect asymmetry induced by relativistic beaming," *Astronomy & Astrophysics*, vol. 686, 2024, doi: 10.1051/0004-6361/202348413